AIMS Mathematics

http://www.aimspress.com/journal/Math

AIMS Mathematics, 6(11): 12395–12421.
DOI:10.3934/math.2021717
Received: 13 March 2021
Accepted: 26 July 2021
Published: 30 August 2021

Research article

On the Caputo-Fabrizio fractal fractional representation for the Lorenz chaotic system

Anastacia Dlamini*, Emile F. Doungmo Goufo and Melusi Khumalo

Department of Mathematical Sciences, University of South Africa, Florida, 0003, South Africa

* **Correspondence:** Email: dlamia@unisa.ac.za.

Abstract: The widespread application of chaotic dynamical systems in different fields of science and engineering has attracted the attention of many researchers. Hence, understanding and capturing the complexities and the dynamical behavior of these chaotic systems is essential. The newly proposed fractal-fractional derivative and integral operators have been used in literature to predict the chaotic behavior of some of the attractors. It is argued that putting together the concept of fractional and fractal derivatives can help us understand the existing complexities better since fractional derivatives capture a limited number of problems and on the other side fractal derivatives also capture different kinds of complexities. In this study, we use the newly proposed Caputo-Fabrizio fractal-fractional derivatives and integral operators to capture and predict the behavior of the Lorenz chaotic system for different values of the fractional dimension q and the fractal dimension k. We will look at the well-posedness of the solution. For the effect of the Caputo-Fabrizio fractal-fractional derivatives operator on the behavior, we present the numerical scheme to study the graphical numerical solution for different values of q and k.

Keywords: Caputo-Fabrizio fractal-fractional derivatives and integral operators; Lorenz chaotic system; well-posedness; Adams-Bashforth method
Mathematics Subject Classification: 26A33, 34A08, 34B15

1. Introduction

The complexities of physical phenomena in nature have forced researchers into developing mathematical models that can be used to describe and capture the behavior of these natural occurrences. Traditional calculus may seem to be enough in solving problems that arise from science and engineering. However, many physical phenomena may better be described by fractional calculus because it is a well-suited tool to analyze problems of fractal dimension, with long term "memory" and chaotic behavior [1]. Some of the advantages of using fractional calculus over classical calculus

are presented by authors in [2–5]. Even though fractional calculus was initially a pure mathematics idea and now regarded as a part of applied mathematics, its application has spread to other fields such as physics [3, 6], economy [4], biology [3, 5, 7–10], probability [11], signal processing [12], quantitative biology, elasticity, diffusion process, systems identification, viscoelasticity [13], transport theory, electrochemistry, rheology, control theory, potential theory, and scattering theory [14, 15]. Many authors have looked at the theoretical results based on the well-posedness of the fractional differential equations in different forms [16–19]. It is clear that for most fractional differential problems, analytical solutions are either impossible to find or are only possible under unrealistic simplifications. As a result, different numerical techniques have been presented by many authors, among which are the variational iteration method, finite difference schemes, Adomain's decomposition, Fourier spectral methods, homotopy analysis methods, A two-step Adams-Bashforth method [20], Haar wavelet numerical method [21], and many others that have been presented in [22].

Another concept that has raised interest in researchers is chaotic systems. Chaotic behavior can be seen in a variety of systems such as fluid dynamics [23], population growth, the dynamics of molecular vibration, ecology, electric circuits, the time evolution of the magnetic field of celestial bodies, weather, mechanical devices, and laser [24]. Some of the applications of fractional calculus on systems that exhibit chaotic behavior are presented in [25–30]. In this study, we will consider a three-dimensional nonlinear chaotic system called the Lorenz chaotic system [31–33] introduced by Lorenz [34]. This chaotic system opened doors to the development of many other three-dimensional nonlinear chaotic systems such as stretch-twist-fold flow [30,35], Chen system [36], Rossler system [37] and Lui system [38].

Recently a new concept of differential and integral operators called fractal-fractional differential and integral operators were introduced by Atangana [39], as the convolution of the generalized Mittag-Leffler law, exponential law, and power-law with fractal derivative. These operators consist of two orders, firstly the fractional-order q then the fractal dimension k. The purpose of the new operators is to attract nonlocal problems in nature that also display fractal behavior. The fractal-fractional derivatives find their applications in long-term relation description, macro, and micro-scaled phenomena, discontinuous differential problems, anomalous physical processes [40–42]. Many authors have looked and these operators and applied them to different fields. Authors such as Qureshi and Atangana [43] presented a paper where they used fractal-fractional differentiation to model and analyzed mathematically the dynamics of the transmission of diarrhea that occurred in Ghana between the year 2008 and 2018. A similar study was done by Srivastava, and Saad [44]. In their case, they used fractional fractal operators to model the ebola virus. The idea of modeling using fractal fractional derivative was also used by Atangana et al. [16] for fractional reaction-diffusion equations. Atangana and Qureshi [45] presented a paper where they used the fractional fractal operators to predict chaotic behavior of the Modified Lu Chen attractor, Modified Chua chaotic attractor, Lu Chen attractor, and Chen attractor.

The rest of this paper is arranged in the following way. Under Section 2, we briefly discuss some of the properties and definitions used in this study. The Lorenz Chaotic system under the fractal fractional Caputo Fabrizio derivative is presented in Section 3. In Section 4, we look at the well-posedness of the solution. The numerical scheme is derived in 5. The numerical simulation and graphical results are presented in Section 6. Numerical discussion and error estimate in Sections 7. Lastly, the conclusion is in found Section 8.

2. Preliminaries

In this section, we will give a brief discussion of some important definitions and properties from fractal-fractional calculus that are useful for this paper.

The following definitions are discussed in detail in [39].

Definition 2.1. [39] Suppose that $u(t)$ is a continuous function and fractal differentiable on an open interval (a, b) with order k then, a q order fractal-fractional derivative of the function $u(t)$ in a Caputo sense with a power-law type kernel is given by:

$$D_{a,t}^{q,k}(u(t)) = \frac{1}{\Gamma(n-q)} \int_a^t \frac{du(s)}{ds^k}(t-s)^{n-q-1} ds, \tag{2.1}$$

where $0 < n - 1 < q, k \leq n \in \mathbb{N}$ and

$$\frac{du(s)}{ds^k} = \lim_{t \to s} \frac{u(x) - u(s)}{t^k - s^k}.$$

A generalized version of the above equation is defined as follows:

$$D_{a,t}^{q,k,\theta}(u(t)) = \frac{1}{\Gamma(n-q)} \int_a^t \frac{d^\theta u(s)}{ds^k}(t-s)^{n-q-1} ds, \tag{2.2}$$

and

$$\frac{d^\theta u(s)}{ds^k} = \lim_{t \to s} \frac{u^\theta(x) - u^\theta(s)}{t^k - s^k},$$

where $\theta \leq 1$.

Definition 2.2. [39] Suppose that $u(t)$ is a continuous function and fractal differentiable on an open interval (a, b) with order k then, a q order fractal-fractional derivative of the function $u(t)$ in a Caputo sense with an exponential decay type kernel is given by:

$$D_{a,t}^{q,k}(u(t)) = \frac{M(q)}{1-q} \int_a^t \frac{du(s)}{ds^k} \exp\Big[- \frac{q}{1-q}(t-s)\Big] ds, \tag{2.3}$$

where $0 < q, k \leq n \in \mathbb{N}$ and $M(0) = M(1) = 1$.
A generalized version of the above equation is defined as follows:

$$D_{a,t}^{q,k,\theta}(u(t)) = \frac{M(q)}{1-q} \int_a^t \frac{d^\theta u(s)}{ds^k} \exp\Big[- \frac{q}{1-q}(t-s)\Big] ds, \tag{2.4}$$

where $0 < q, k, \theta \leq 1$.

Definition 2.3. [39] Suppose that $u(t)$ is a continuous function and fractal differentiable on an open interval (a, b) with order k then, a q order fractal-fractional derivative of the function $u(t)$ in a Caputo sense with the generalized Mittag-Leffler kernel is given by:

$$D_{a,t}^{q,k}(u(t)) = \frac{AB(q)}{1-q}\int_a^t \frac{du(s)}{ds^k} E_q\Big(-\frac{q}{1-q}(t-s)^q\Big)ds, \tag{2.5}$$

A generalized version of the above equation is defined as follows:

$$D_{a,t}^{q,k,\theta}(u(t)) = \frac{AB(q)}{1-q}\int_a^t \frac{d^\theta u(s)}{ds^k} E_q\Big(-\frac{q}{1-q}(t-s)^q\Big)ds, \tag{2.6}$$

where $0 < \alpha, \beta \leq 1$ and $AB(\alpha) = 1 - \alpha + \dfrac{\alpha}{\Gamma(\alpha)}$.

Definition 2.4. [39] Suppose that $u(t)$ is a continuous function and fractal differentiable on an open interval (a, b) with order k then, a q order fractal-fractional derivative of the function $u(t)$ in a Caputo sense with exponential decay kernel is given by:

$$D_{a,t}^{q,k}(u(t)) = \frac{M(q)}{(1-q)}\frac{d}{ds^k}\int_a^t u(s)\exp\Big[-\frac{q}{1-q}(t-s)^2\Big]ds, \tag{2.7}$$

where $0 < q, k \leq n$ and $M(0) = M(1) = 1$.
A generalized version of the above equation is defined as follows:

$$D_{a,t}^{q,k,\theta}(u(t)) = \frac{M(q)}{(1-q)}\frac{d^\theta}{ds^k}\int_a^t u(s)\exp\Big[-\frac{q}{1-q}(t-s)^2\Big]ds, \tag{2.8}$$

where $0 < q, k, \theta \leq 1$.

Definition 2.5. [39] Assuming that $u(t)$ is a continuous function on (a, b) , then a q order fractal-fractional integral of the function $u(t)$ with power law type kernel is given by:

$$J_{a,t}^{q,k}(u(t)) = \frac{k}{\Gamma(q)}\int_a^t (t-s)^{q-1}s^{k-1}u(s)ds. \tag{2.9}$$

Definition 2.6. [39] Assuming that $u(t)$ is a continuous function on (a, b) , then a q order fractal-fractional integral of the function $u(t)$ with an exponential decaying type kernel is given by:

$$J_{a,t}^{q,k}(u(t)) = \frac{qk}{M(q)}\int_a^t s^{q-1}u(s)ds + \frac{k(1-q)t^{k-1}u(t)}{M(q)}. \tag{2.10}$$

Definition 2.7. [39] Assuming that $u(t)$ is a continuous function on (a, b), then a q order fractal-fractional integral of the function $u(t)$ with a generalized Mittag-Leffler type kernel is given by:

$$J_{a,t}^{q,k}(u(x)) = \frac{qk}{AB(q)}\int_a^t s^{k-1}u(s)(t-s)^{q-1}ds + \frac{k(1-q)t^{k-1}u(t)}{AB(q)}. \tag{2.11}$$

3. The Lorenz chaotic system under the fractal fractional Caputo-Fabrizio derivative

In this section, we introduce the Lorenz chaotic system under the definition of fractal fractional Caputo-Fabrizio derivative.

Consider the following three dimensional nonlinear chaotic system called the Lorenz chaotic system [24, 46]

$$\begin{aligned} x'(t) &= \gamma(y - x), \\ y'(t) &= \rho x - y - xz, \\ z'(t) &= xy - \delta z, \end{aligned} \tag{3.1}$$

where $x = x(t)$, $y = y(t)$, and $z = z(t)$ are the dynamical variable of the system and γ, ρ, and δ are the related real constants parameters. Using the definition of the fractal-fractional derivative under the Riemann-Liouville sense with exponential decay kernel for each classical derivative equations in (3.1), we obtain

$$\begin{aligned} {}^{RL}D_{0,t}^{q,k}x(t) &= \Phi_1(x, y, z, t), \\ {}^{RL}D_{0,t}^{q,k}y(t) &= \Phi_2(x, y, z, t), \\ {}^{RL}D_{0,t}^{q,k}z(t) &= \Phi_3(x, y, z, t), \end{aligned} \tag{3.2}$$

where $\Phi_1(x, y, z, t) = \gamma(y - x)$, $\Phi_2(x, y, z, t) = \rho x - y - xz$, and $\Phi_3(x, y, z, t) = xy - \delta z$. The above system of equations can be written as follows

$$\begin{aligned} {}^{RL}D_{0,t}^{q,k}x(t) &= \frac{M(q)}{1-q}\frac{d}{dt^k}\int_0^t \exp\Big(-\frac{q}{1-q}(t-s)\Big)\Phi_1(x, y, z, s)ds, \\ {}^{RL}D_{0,t}^{q,k}y(t) &= \frac{M(q)}{1-q}\frac{d}{dt^k}\int_0^t \exp\Big(-\frac{q}{1-q}(t-s)\Big)\Phi_2(x, y, z, s)ds, \\ {}^{RL}D_{0,t}^{q,k}z(t) &= \frac{M(q)}{1-q}\frac{d}{dt^k}\int_0^t \exp\Big(-\frac{q}{1-q}(t-s)\Big)\Phi_3(x, y, z, s)ds. \end{aligned} \tag{3.3}$$

Since the fractional integral is differentiable. We can rewrite the Eq (3.3) as

$$\begin{aligned} {}^{RL}D_{0,t}^{q,k}x(t) &= \frac{M(q)}{1-q}\frac{d}{dt}\int_0^t \exp\Big(-\frac{q}{1-q}(t-s)\Big)\Phi_1(x, y, z, s)ds\frac{1}{kt^{k-1}}, \\ {}^{RL}D_{0,t}^{q,k}y(t) &= \frac{M(q)}{1-q}\frac{d}{dt}\int_0^t \exp\Big(-\frac{q}{1-q}(t-s)\Big)\Phi_2(x, y, z, s)ds\frac{1}{kt^{k-1}}, \\ {}^{RL}D_{0,t}^{q,k}z(t) &= \frac{M(q)}{1-q}\frac{d}{dt}\int_0^t \exp\Big(-\frac{q}{1-q}(t-s)\Big)\Phi_3(x, y, z, s)ds\frac{1}{kt^{k-1}}. \end{aligned} \tag{3.4}$$

Therefore, system (3.4) can be expressed as follows

$${}^{RL}D_{0,t}^{q,k}x(t) = kt^{k-1}\Phi_1(x, y, z, t),$$

$$
\begin{aligned}
{}^{RL}D_{0,t}^{q,k}y(t) &= kt^{k-1}\Phi_2(x,y,z,t),\\
{}^{RL}D_{0,t}^{q,k}z(t) &= kt^{k-1}\Phi_3(x,y,z,t).
\end{aligned}
\tag{3.5}
$$

We now replace the Riemann-Liouville derivative with the Caputo-Fabrizio derivative to make use of the integer-order initial conditions. Thus from system (3.5) we get

$$
\begin{aligned}
{}^{CF}D_{0,t}^{q,k}x(t) &= kt^{k-1}\Phi_1(x,y,z,t),\\
{}^{CF}D_{0,t}^{q,k}y(t) &= kt^{k-1}\Phi_2(x,y,z,t),\\
{}^{CF}D_{0,t}^{q,k}z(t) &= kt^{k-1}\Phi_3(x,y,z,t).
\end{aligned}
\tag{3.6}
$$

In this study, we will investigate the above system of equations.

4. The well-posedness of the fractal fractional Caputo-Frabrizio derivative of the Lorenz system

In this section, we use the Pichard Lindelof method [46–48] to show the existence and uniqueness of the solution of the following nonlinear system of equations

$$
\begin{aligned}
{}^{CF}D_{0,t}^{q,k}x(t) &= kt^{k-1}\Phi_1(x,y,z,t),\\
{}^{CF}D_{0,t}^{q,k}y(t) &= kt^{k-1}\Phi_2(x,y,z,t),\\
{}^{CF}D_{0,t}^{q,k}z(t) &= kt^{k-1}\Phi_3(x,y,z,t),
\end{aligned}
\tag{4.1}
$$

subjected to the following initial conditions

$$
\begin{aligned}
x(0) &= x_0,\\
y(0) &= y_0,\\
z(0) &= z_0.
\end{aligned}
$$

To show the existence and uniqueness of the solution we define the following operators.

$$
\begin{aligned}
f_1(t,x) &= \gamma(y-x),\\
f_2(t,y) &= \rho x - y - xz,\\
f_3(t,z) &= xy - \delta z,
\end{aligned}
\tag{4.2}
$$

Now, let

$$
\begin{aligned}
C_{a,b_1} &= A_1 \times B_1,\\
C_{a,b_2} &= A_2 \times B_2,\\
C_{a,b_3} &= A_3 \times B_3,
\end{aligned}
\tag{4.3}
$$

where

$$\begin{aligned} A_1 &= A_2 = A_3 = [t_0 - a, t_0 + a], \\ B_1 &= [x_0 - b_1, x_0 + b_1], \\ B_2 &= [y_0 - b_2, y_0 + b_2], \\ B_3 &= [z_0 - b_3, z_0 + b_3], \end{aligned} \tag{4.4}$$

We now want to show that f_1, f_2 and f_3 satisfy the Lipschipitz conditions with respect to x, y, z respectively. This means that for any two given functions $\psi_1, \psi_2 \in C(A_1, B_1, B_2, B_3)$ there exists a positive constant k such that

$$\left\| f(t, \psi_1) - f(t, \psi_2) \right\| \leq k \left\| \psi_1 - \psi_2 \right\|.$$

For f_1 we have

$$\begin{aligned} \left\| f_1(t, \psi_1) - f_1(t, \psi_2) \right\| &= \left\| (\gamma y(t) - \gamma \psi_1)) - (\gamma y(t) - \gamma \psi_2) \right\| \\ &= \left\| - \gamma \psi_1 + \gamma \psi_2 \right\| \\ &= \left\| - \gamma (\psi_1 - \psi_2) \right\| \\ &\leq |\gamma| \left\| \psi_1 - \psi_2 \right\|. \end{aligned} \tag{4.5}$$

Hence, f_1 is satisfies the Lipschipitz conditions. For f_2 we have

$$\begin{aligned} \left\| f_2(t, \psi_1) - f_2(t, \psi_2) \right\| &= \left\| (\rho x(t) - \psi_1 - x(t) z(t)) - (\rho x(t) - \psi_2 - x(t) z(t)) \right\| \\ &= \left\| - \psi_1 + \psi_2 \right\| \\ &= \left\| - (\psi_1 - \psi_2) \right\| \\ &\leq \left\| \psi_1 - \psi_2 \right\|. \end{aligned} \tag{4.6}$$

Thus, f_2 is satisfies the Lipschipitz conditions. For f_3 we have

$$\begin{aligned} \left\| f_3(t, \psi_1) - f_3(t, \psi_2) \right\| &= \left\| (x(t) y(t) - \delta \psi_1) - (x(t) y(t) - \delta \psi_2)) \right\| \\ &= \left\| - \delta \psi_1 + \delta \psi_2 \right\| \\ &= \left\| - \delta (\psi_1 - \psi_2) \right\| \\ &\leq |\delta| \left\| \psi_1 - \psi_2 \right\|. \end{aligned} \tag{4.7}$$

Therefore, f_3 satisfies the Lipschipitz conditions.

Now, let

$$M_1 = \sup_{C_{a,b_1}} |f_1(t, x)|,$$

$$M_2 = \sup_{C_{a,b_2}} |f_2(t,y)|, \tag{4.8}$$
$$M_3 = \sup_{C_{a,b_3}} |f_3(t,z)|,$$

We now continue to apply the Banach fixed point theorem using the metric on spaces of continuous functions $C(A_1, B_1, B_2, B_3)$ induced by the norm

$$\left\|f(t)\right\|_\infty = \sup_{t\in[t_0-a,t_0+a]} |f(t)|. \tag{4.9}$$

We now define the next operator between the two functional spaces of continuous functions, Picard's operator, as follows

$$D : C(A_1, B_1, B_2, B_3) \to C(A_1, B_1, B_2, B_3). \tag{4.10}$$

Defined as follows

$$DX(t) = X_0(t) + \frac{kt^{k-1}(1-q)}{M(q)}F(t, X(t)) + \frac{qk}{M(q)}\int_0^t \Lambda^{\tau-1}F(\Lambda, X(\Lambda))d\Lambda \tag{4.11}$$

Where the matrix X is given as

$$X(t) = \begin{bmatrix} x(t) \\ y(t) \\ z(t) \end{bmatrix}$$

$$X_0(t) = \begin{bmatrix} x_0 \\ y_0 \\ z_0 \end{bmatrix}$$

and

$$F(t, X(t)) = \begin{bmatrix} f_1(t,x) \\ f_2(t,y) \\ f_3(t,z) \end{bmatrix}$$

From (4.5)–(4.7) we can conclude that $F(t, X(t))$ satisfies Lipschipitz conditions with respect to the system state variable $X(t)$. Now, we must show that this operator maps a complete nonempty space

into itself. We first show that, given a certain restriction on a, D takes values in B_1, B_2, B_3 in the space of continuous functions with uniform norm. To obtain good results, we assume that the problem under consideration satisfies

$$\|X(t)\|_\infty = \max\{b_1, b_2, b_3\} = b$$

implies

$$\begin{aligned}
\left\|DX(t) - X_0(t)\right\| &= \left\|\frac{kt^{k-1}(1-q)}{M(q)}F(t, X(t)) + \frac{qk}{M(q)}\int_0^t \Lambda^{k-1}F(\Lambda, X(\Lambda))d\Lambda\right\| \\
&\leq \frac{kt^{k-1}(1-q)}{M(q)}\left\|F(t, X(t))\right\| + \frac{qk}{M(q)}\int_0^t \Lambda^{k-1}\left\|F(\Lambda, X(\Lambda))d\Lambda\right\| \\
&\leq \frac{kt^{k-1}(1-q)}{M(q)}M + \frac{qk}{M(q)}.\frac{Ma^k}{k} \\
&\leq Ma \\
&\leq b,
\end{aligned} \tag{4.12}$$

where $b = \max\{b_1, b_2, b_3\}$ and $M = \max\{M_1, M_2, M_3\}$. The last step is true if we impose the requirement $a < \frac{b}{M}$.

Using the maximum's metric

$$\left\|DX_1 - DX_2\right\|_\infty = \sup_{t\in[t_0-a,t_0+a]} |X_1 - X_2|. \tag{4.13}$$

We want to show that the operator is a contraction mapping. So, we have

$$\begin{aligned}
\left\|DX(t) - X_0(t)\right\| &= \left\|\frac{t^{k-1}(1-q)}{M(q)}[F(t, X_1(t)) - F(t, X_2(t))]\right. \\
&\quad \left. + \frac{qk}{M(q)}\int_0^t \Lambda^{k-1}[F(\Lambda, X_1(\Lambda)) - F(\Lambda, X_2(\Lambda))]d\Lambda\right\| \\
&\leq \frac{kt^{k-1}(1-q)}{M(q)}\left\|F(t, X_1(t)) - F(t, X_2(t))\right\| \\
&\quad + \frac{qk}{M(q)}\int_0^t \lambda^{k-1}\left\|F(\Lambda, X_1(\Lambda)) - F(\Lambda, X_2(\Lambda))\right\|d\Lambda \\
&\leq \frac{kt^{k-1}(1-q)}{M(q)}p\left\|X_1(t) - X_2(t)\right\| + \frac{qk}{M(q)}\int_0^t \Lambda^{k-1}\left\|F(\Lambda, X_1(\Lambda)) - F(\Lambda, X_2(\Lambda))\right\|d\Lambda
\end{aligned}$$

F is Lipschitz continuous

$$\begin{aligned}
&\leq \frac{kt^{k-1}(1-q)}{M(q)}p\left\|X_1(t) - X_2(t)\right\| + \frac{qa^kp}{M(q)}\left\|X_1(t) - X_2(t)\right\| \\
&= \left(\frac{pkt^{k-1}(1-q)}{M(q)} + \frac{qa^kp}{M(q)}\right)\left\|X_1(t) - X_2(t)\right\|
\end{aligned}$$

$$\leq ap\left\|X_1(t) - X_2(t)\right\| \tag{4.14}$$

with $p < 1$. Since F is Lipschitz continuous, we have that the operator D is a contraction for $arp < 1$. Hence, this shows that the system under consideration has a unique set of solution.

5. Numerical scheme

In this section, we present the numerical scheme for the Caputo Fabrizio fractal fractional derivative of the Lorenz chaotic system. The chaotic model (3.1) can be converted to

$$\begin{aligned} {}^{CF}D_{0,t}^{q,k}x(t) &= kt^{k-1}\Phi_1(x, y, z, t), \\ {}^{CF}D_{0,t}^{q,k}y(t) &= kt^{k-1}\Phi_2(x, y, z, t), \\ {}^{CF}D_{0,t}^{q,k}z(t) &= kt^{k-1}\Phi_3(x, y, z, t). \end{aligned} \tag{5.1}$$

Where

$$\begin{aligned} \Phi_1(x, y, z, t) &= \gamma(y - x), \\ \Phi_2(x, y, z, t) &= \rho x - y - xz, \\ \Phi_2(x, y, z, t) &= xy - \delta z. \end{aligned}$$

When we apply the Caputo-Fabrizio integral to (5.1), we get

$$\begin{aligned} x(t) - x(0) &= \frac{kt^{k-1}(1-q)}{M(q)}\Phi_1(x, y, z, t) + \frac{qk}{M(q)}\int_0^t \Lambda^{k-1}\Phi_1(x, y, z, \Lambda)d\Lambda, \\ y(t) - y(0) &= \frac{kt^{k-1}(1-q)}{M(q)}\Phi_2(x, y, z, t) + \frac{qk}{M(q)}\int_0^t \Lambda^{k-1}\Phi_2(x, y, z, \Lambda)d\Lambda, \\ z(t) - z(0) &= \frac{kt^{k-1}(1-q)}{M(q)}\Phi_3(x, y, z, t) + \frac{qk}{M(q)}\int_0^t \Lambda^{k-1}\Phi_3(x, y, z, \Lambda)d\Lambda. \end{aligned} \tag{5.2}$$

For a positive integer n,the solution of the system of Eq (5.1) at $t = t_{n+1}$ becomes,

$$\begin{aligned} x(t_{n+1}) - x(0) &= \frac{kt_n^{k-1}(1-q)}{M(q)}\Phi_1(x(t_n), y(t_n), z(t_n), t_n) + \frac{qk}{M(q)}\int_0^{t_{n+1}} \Lambda^{k-1}\Phi_1(x, y, z, \Lambda)d\Lambda, \\ y(t_{n+1}) - y(0) &= \frac{kt_n^{k-1}(1-q)}{M(q)}\Phi_2(x(t_n), y(t_n), z(t_n), t_n) + \frac{qk}{M(q)}\int_0^{t_{n+1}} \Lambda^{k-1}\Phi_2(x, y, z, \Lambda)d\Lambda, \\ z(t_{n+1}) - z(0) &= \frac{kt_n^{k-1}(1-q)}{M(q)}\Phi_3(x(t_n), y(t_n), z(t_n), t_n) + \frac{qk}{M(q)}\int_0^{t_{n+1}} \Lambda^{k-1}\Phi_3(x, y, z, \Lambda)d\Lambda. \end{aligned} \tag{5.3}$$

and at $t = t_n$, we obtain

$$x(t_n) - x(0) = \frac{kt_{n-1}^{k-1}(1-q)}{M(q)}\Phi_1(x(t_{n-1}), y(t_{n-1}), z(t_{n-1}), t_{n-1}) + \frac{qk}{M(q)}\int_0^{t_n} \Lambda^{k-1}\Phi_1(x, y, z, \Lambda)d\Lambda,$$

$$y(t_n) - y(0) = \frac{kt_{n-1}^{k-1}(1-q)}{M(q)}\Phi_2(x(t_{n-1}), y(t_{n-1}), z(t_{n-1}), t_{n-1}) + \frac{qk}{M(q)}\int_0^{t_n} \Lambda^{k-1}\Phi_2(x, y, z, \Lambda)d\Lambda, \quad (5.4)$$
$$z(t_n) - z(0) = \frac{kt_{n-1}^{k-1}(1-q)}{M(q)}\Phi_3(x(t_{n-1}), y(t_{n-1}), z(t_{n-1}), t_{n-1}) + \frac{qk}{M(q)}\int_0^{t_n} \Lambda^{k-1}\Phi_3(x, y, z, \Lambda)d\Lambda.$$

Taking the difference between (5.4) and (5.3), we get

$$\begin{aligned}
x(t_{n+1}) - x(t_n) &= \frac{kt_n^{k-1}(1-q)}{M(q)}\Phi_1(x(t_n), y(t_n), z(t_n), t_n) \\
&\quad - \frac{kt_{n-1}^{k-1}(1-q)}{M(q)}\Phi_1(x(t_{n-1}), y(t_{n-1}), z(t_{n-1}), t_{n-1}) \\
&\quad + \frac{qk}{M(q)}\int_{t_n}^{t_{n+1}} \Lambda^{k-1}\Phi_1(x, y, z, \Lambda)d\Lambda, \\
y(t_{n+1}) - y(t_n) &= \frac{kt_n^{k-1}(1-q)}{M(q)}\Phi_2(x(t_n), y(t_n), z(t_n), t_n) \\
&\quad - \frac{kt_{n-1}^{k-1}(1-q)}{M(q)}\Phi_2(x(t_{n-1}), y(t_{n-1}), z(t_{n-1}), t_{n-1}) \\
&\quad + \frac{qk}{M(q)}\int_{t_n}^{t_{n+1}} \Lambda^{k-1}\Phi_1(x, y, z, \Lambda)d\Lambda, \quad (5.5) \\
z(t_{n+1}) - z(t_n) &= \frac{kt_n^{k-1}(1-q)}{M(q)}\Phi_3(x(t_n), y(t_n), z(t_n), t_n) \\
&\quad - \frac{kt_{n-1}^{k-1}(1-q)}{M(q)}\Phi_3(x(t_{n-1}), y(t_{n-1}), z(t_{n-1}), t_{n-1}) \\
&\quad + \frac{qk}{M(q)}\int_{t_n}^{t_{n+1}} \Lambda^{k-1}\Phi_3(x, y, z, \Lambda)d\Lambda.
\end{aligned}$$

We now approximate the functions $\Lambda^{k-1}\Phi_1(x, y, z, \Lambda)$, $\Lambda^{k-1}\Phi_2(x, y, z, \Lambda)$ and $\Lambda^{k-1}\Phi_3(x, y, z, \Lambda)$ on the finite interval $[t_n, t_{n+1}]$ using the piece-wise Lagrangian interpolation such as

$$\begin{aligned}
Q_1(\Lambda) &= \frac{\Lambda - t_{n-1}}{t_n - t_{n-1}}t_n^{k-1}\Phi_1(x(t_n), y(t_n), z(t_n), t_n) - \frac{\Lambda - t_n}{t_n - t_{n-1}}t_{n-1}^{k-1}\Phi_1(x(t_{n-1}), y(t_{n-1}), z(t_{n-1}), t_{n-1}), \\
Q_2(\Lambda) &= \frac{\Lambda - t_{n-1}}{t_n - t_{n-1}}t_n^{k-1}\Phi_2(x(t_n), y(t_n), z(t_n), t_n) - \frac{\Lambda - t_n}{t_n - t_{n-1}}t_{n-1}^{k-1}\Phi_2(x(t_{n-1}), y(t_{n-1}), z(t_{n-1}), t_{n-1}), \\
Q_3(\Lambda) &= \frac{\Lambda - t_{n-1}}{t_n - t_{n-1}}t_n^{k-1}\Phi_3(x(t_n), y(t_n), z(t_n), t_n) - \frac{\Lambda - t_n}{t_n - t_{n-1}}t_{n-1}^{k-1}\Phi_3(x(t_{n-1}), y(t_{n-1}), z(t_{n-1}), t_{n-1}). \quad (5.6)
\end{aligned}$$

Substituting (5.6) into (5.5) and integrating, we obtain

$$\begin{aligned}
x(t_{n+1}) - x(t_n) &= kt_n^{k-1}\Big(\frac{3q\triangle t}{2M(q)} + \frac{(1-q)}{M(q)}\Big)\Phi_1(x(t_n), y(t_n), z(t_n), t_n) \\
&\quad - kt_{n-1}^{k-1}\Big(\frac{q\triangle t}{2M(q)} + \frac{(1-q)}{M(q)}\Big)\Phi_1(x(t_{n-1}), y(t_{n-1}), z(t_{n-1}), t_{n-1}),
\end{aligned}$$

$$
\begin{aligned}
y(t_{n+1}) - y(t_n) &= kt_n^{k-1}\Big(\frac{3q\triangle t}{2M(q)} + \frac{(1-q)}{M(q)}\Big)\Phi_2(x(t_n), y(t_n), z(t_n), t_n) \\
&\quad - kt_{n-1}^{k-1}\Big(\frac{q\triangle t}{2M(q)} + \frac{(1-q)}{M(q)}\Big)\Phi_2(x(t_{n-1}), y(t_{n-1}), z(t_{n-1}), t_{n-1}), \qquad (5.7)\\
z(t_{n+1}) - z(t_n) &= kt_n^{k-1}\Big(\frac{3q\triangle t}{2M(q)} + \frac{(1-q)}{M(q)}\Big)\Phi_3(x(t_n), y(t_n), z(t_n), t_n) \\
&\quad - kt_{n-1}^{k-1}\Big(\frac{q\triangle t}{2M(q)} + \frac{(1-q)}{M(q)}\Big)\Phi_3(x(t_{n-1}), y(t_{n-1}), z(t_{n-1}), t_{n-1}),
\end{aligned}
$$

Therefore, we have completed the derivation of the numerical scheme used in this study.

6. Numerical simulation

In the previous section, we presented a numerical scheme under the Caputo-Fabrizio fractal-fractional derivative operator. In this section, we aim to use the numerical scheme presented to approximate the graphical solution for the Lorenz chaotic systems under the Caputo-Fabrizio fractal-fractional derivative operator for different values of the fractional dimension q and the fractal dimension k. We now look at the following examples:

Example 1. Consider the following system of equations

$$
\begin{aligned}
{}^{CF}D_{0,t}^{q,k}x(t) &= kt^{k-1}\Phi_1(x, y, z, t),\\
{}^{CF}D_{0,t}^{q,k}y(t) &= kt^{k-1}\Phi_2(x, y, z, t),\\
{}^{CF}D_{0,t}^{q,k}z(t) &= kt^{k-1}\Phi_3(x, y, z, t),
\end{aligned} \qquad (6.1)
$$

where $\Phi_1(x, y, z, t) = \gamma(y - x)$, $\Phi_2(x, y, z, t) = \rho x - y - xz$, and $\Phi_2(x, y, z, t) = xy - \delta z$. With parameter values $\gamma = 10$, $\rho = 28$ and $\delta = \frac{8}{3}$. In this example we solve the system (6.1) using the initial conditions $x(0) = y(0) = z(0) = -1$. The graphical numerical simulations for different values of q and k for this example are presented in Figures 1–4.

Example 2. For the the second example, we consider the system of equation in example 1 with different initial conditions. Consider the following system of equations

$$
\begin{aligned}
{}^{CF}D_{0,t}^{q,k}x(t) &= kt^{k-1}\Phi_1(x, y, z, t),\\
{}^{CF}D_{0,t}^{q,k}y(t) &= kt^{k-1}\Phi_2(x, y, z, t),\\
{}^{CF}D_{0,t}^{q,k}z(t) &= kt^{k-1}\Phi_3(x, y, z, t).
\end{aligned} \qquad (6.2)
$$

In this example, we solve the system (6.2) using the initial conditions $x(0) = 0$, $y(0) = 2$ and $z(0) = 20$. The graphical numerical simulations for different values of q and k for this example are presented in Figures 5–8.

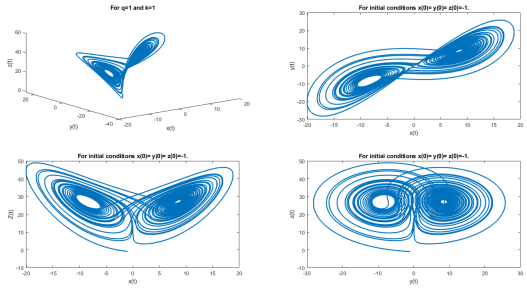

(a) For $q = 1$ and $k = 1$ (Example 1).

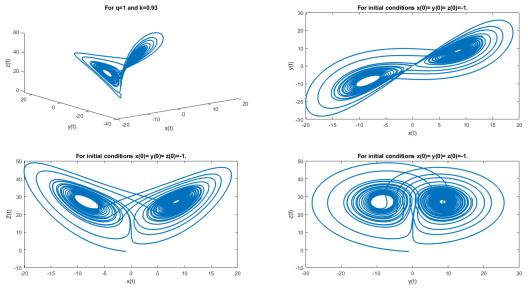

(b) For $q = 1$ and $k = 0.93$ (Example 1).

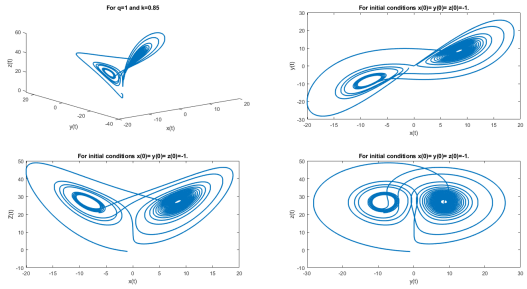

(c) For $q = 1$ and $k = 0.85$ (Example 1).

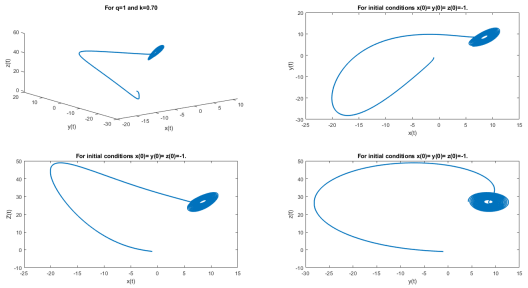

(d) For $q = 1$ and $k = 0.70$ (Example 1).

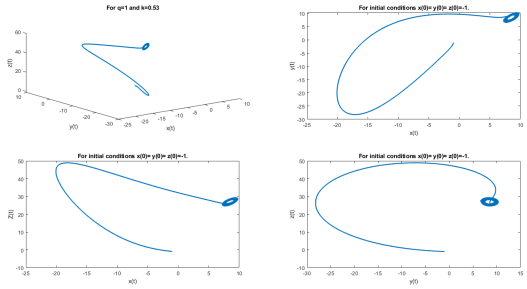

(e) For $q = 1$ and $k = 0.53$ (Example 1).

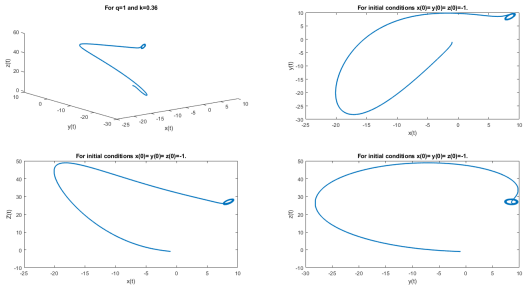

(f) For $q = 1$ and $k = 0.36$ (Example 1).

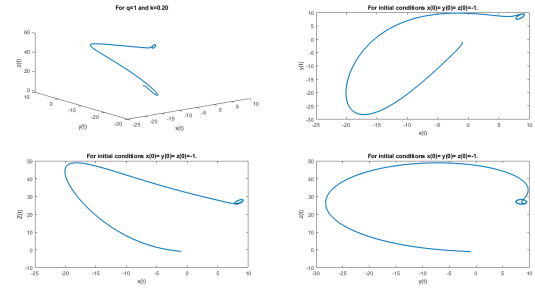

(g) For $q = 1$ and $k = 0.20$ (Example 1).

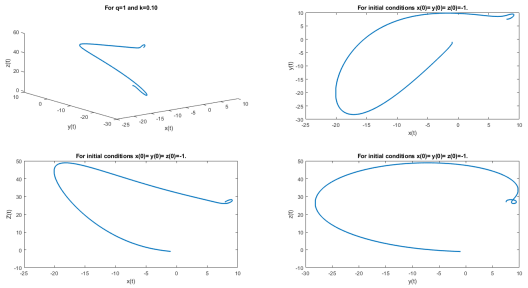

(h) For $q = 1$ and $k = 0.10$ (Example 1).

Figure 1. The dynamical behavior of the Lorenz chaotic system (6.1), using the Caputo-Fabrizio fractal-fractional derivative operator for different values of k and q.

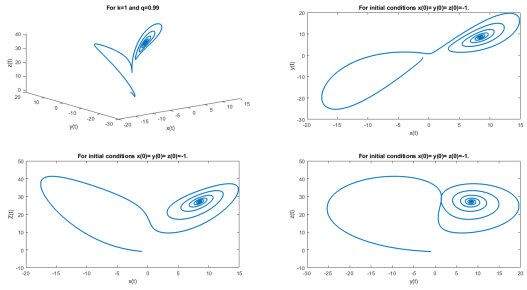

(a) For $k = 1$ and $q = 0.99$ (Example 1).

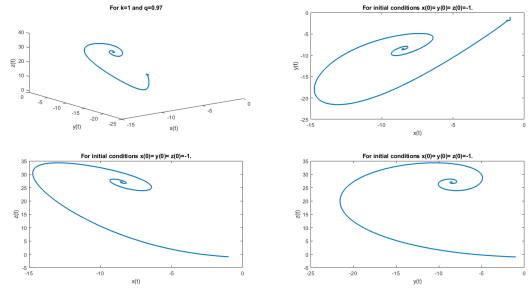

(b) For $k = 1$ and $q = 0.98$ (Example 1).

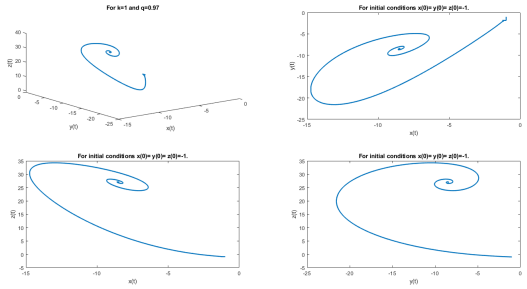

(c) For $k = 1$ and $q = 0.97$ (Example 1).

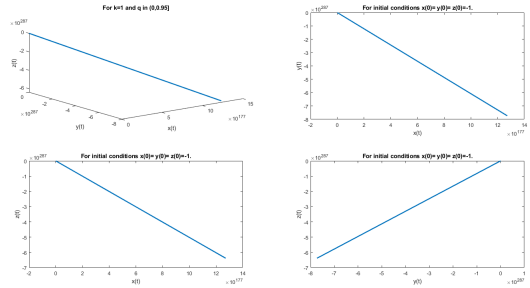

(d) For $k = 1$ and $0 < q \leq 0.95$ (Example 1).

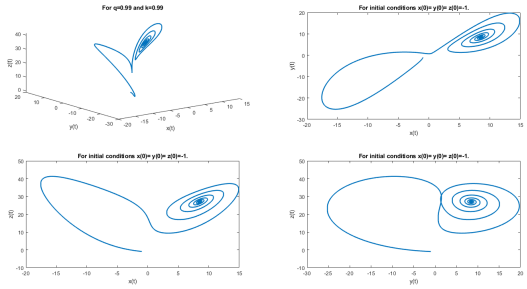

(e) For $q = 0.99$ and $k = 0.99$ (Example 1).

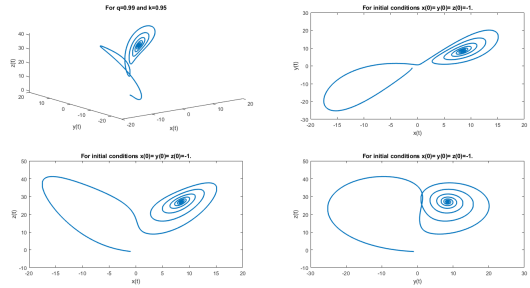

(f) For $q = 0.99$ and $k = 0.95$ (Example 1).

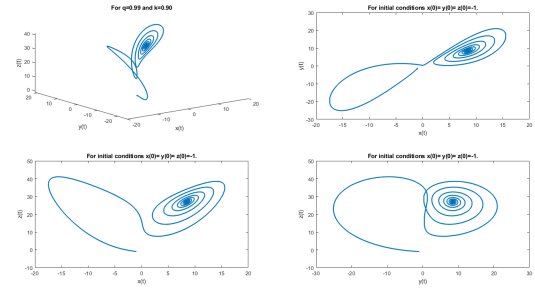

(g) For $q = 0.99$ and $k = 0.90$ (Example 1).

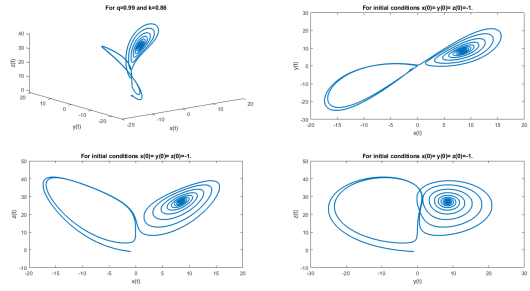

(h) For $q = 0.99$ and $k = 0.86$ (Example 1).

Figure 2. The dynamical behavior of the Lorenz chaotic system (6.1), using the Caputo-Fabrizio fractal-fractional derivative operator for different values of k and q.

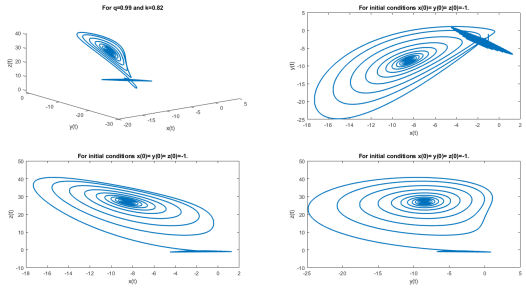

(a) For $q = 0.99$ and $k = 0.82$ (Example 1).

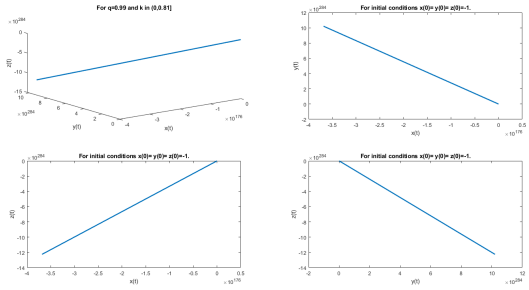

(b) For $q = 0.99$ and $0 < k \leq 0.81$ (Example 1).

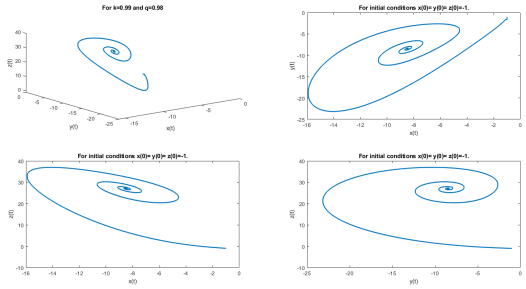

(c) For $k = 0.99$ and $0 < q \leq 0.95$ (Example 1).

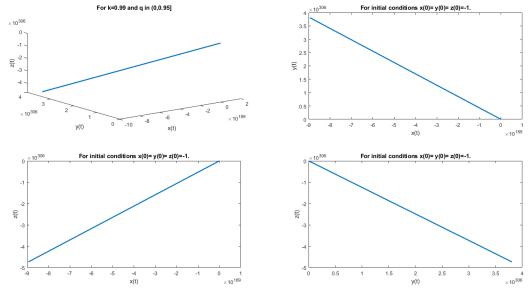

(d) For $k = 0.99$ and $0 < q \leq 0.95$ (Example 1).

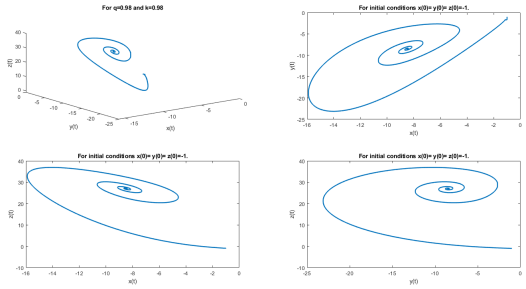

(e) For $q = 0.98$ and $k = 0.98$ (Example 1).

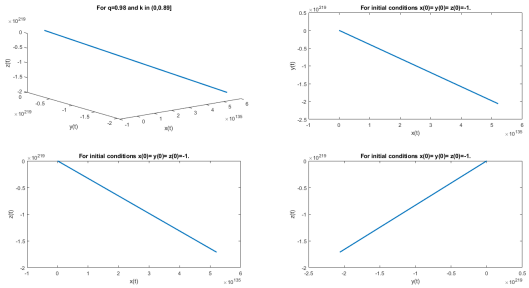

(f) For $q = 0.98$ and $0 < k \leq 0.89$ (Example 1).

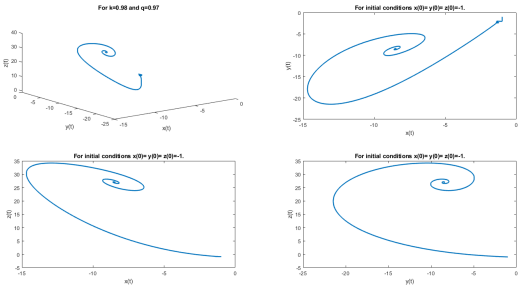

(g) For $k = 0.98$ and $q = 0.97$ (Example 1).

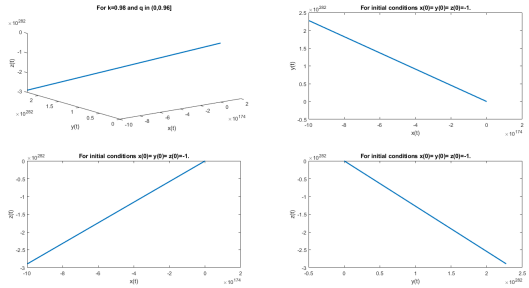

(h) For $k = 0.98$ and $0 < q \leq 0.96$ (Example 1).

Figure 3. The dynamical behavior of the Lorenz chaotic system (6.1), using the Caputo-Fabrizio fractal-fractional derivative operator for different values of k and q.

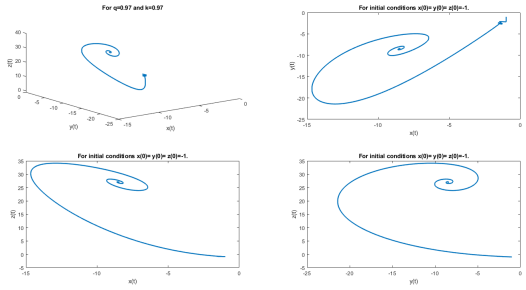

(a) For $q = 0.97$ and $k = 0.97$ (Example 1).

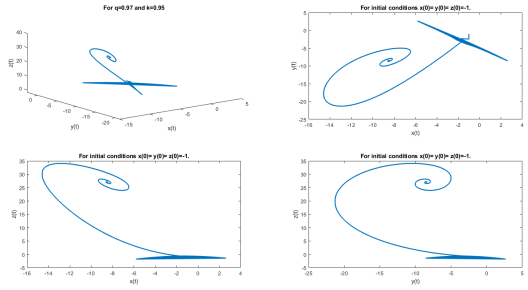

(b) For $q = 0.97$ and $k = 0.95$ (Example 1).

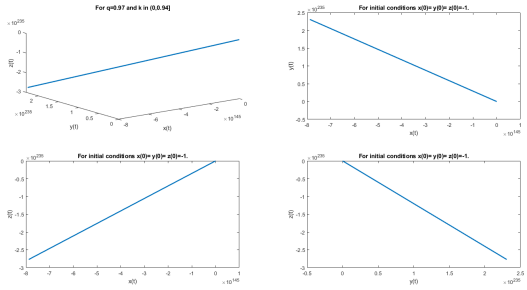

(c) For $q = 0.97$ and $0 < k \leq 0.94$ (Example 1).

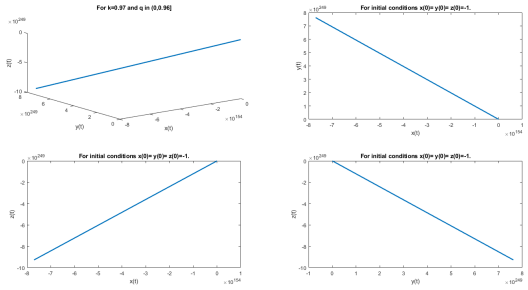

(d) For $k = 0.97$ and $0 < q \leq 0.96$ (Example 1).

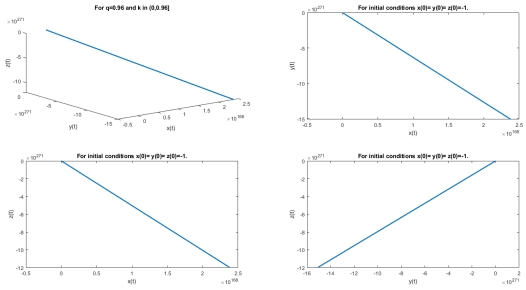

(e) For $q = 0.96$ and $0 < k \leq 0.96$ (Example 1).

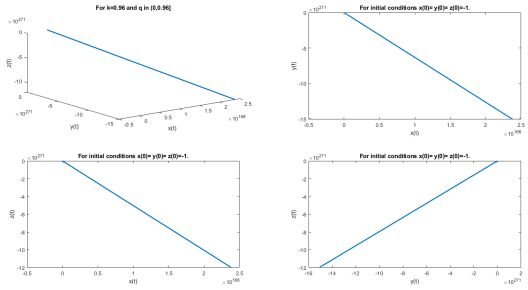

(f) For $k = 0.96$ and $0 < q \leq 0.96$ (Example 1).

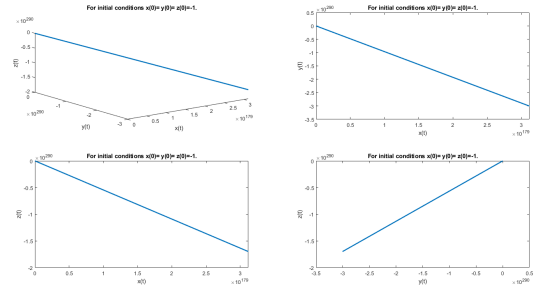

(g) For $0 < q \leq 0.94$ and $0 < k \leq 1$ (Examp 1).

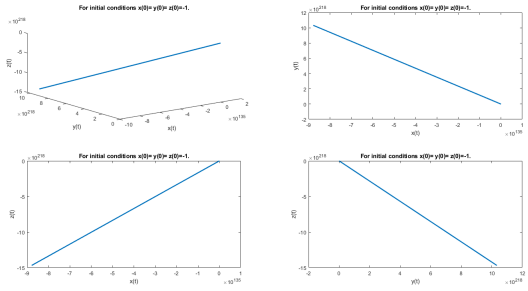

(h) For $0 < k \leq 0.95$and $0 < q \leq 0.96$ (Example 1).

Figure 4. The dynamical behavior of the Lorenz chaotic system (6.1), using the Caputo-Fabrizio fractal-fractional derivative operator for different values of k and q.

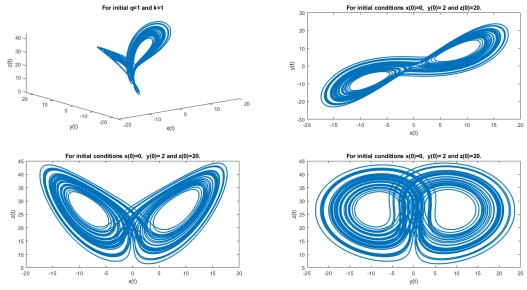

(a) For $q = 1$ and $k = 1$ (Example 2).

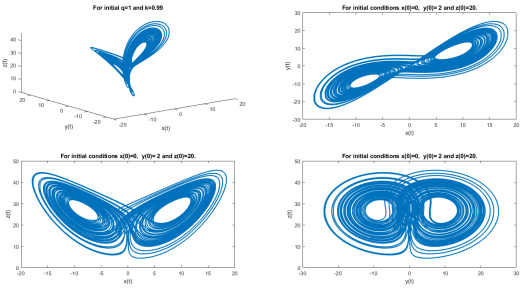

(b) For $q = 1$ and $k = 0.99$ (Example 2).

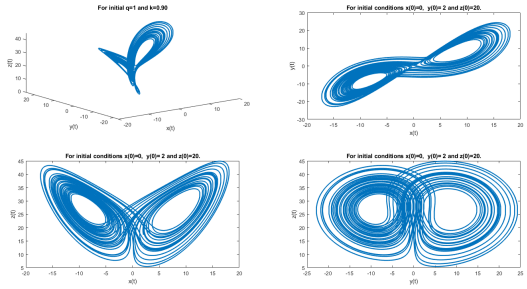

(c) For $q = 1$ and $k = 0.90$ (Example 2).

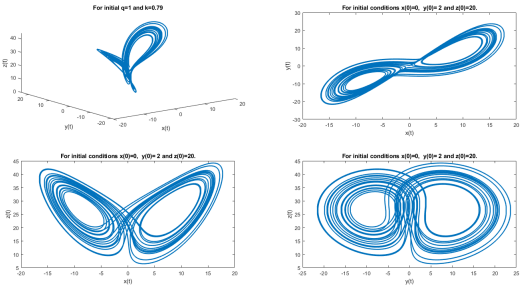

(d) For $q = 1$ and $k = 0.79$ (Example 2).

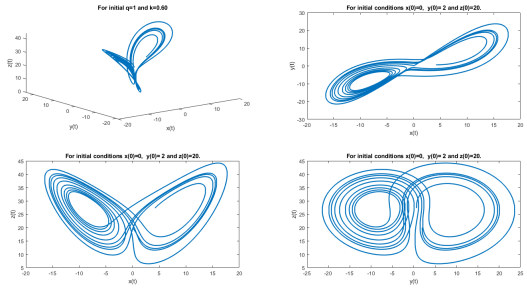

(e) For $q = 1$ and $k = 0.60$ (Example 2).

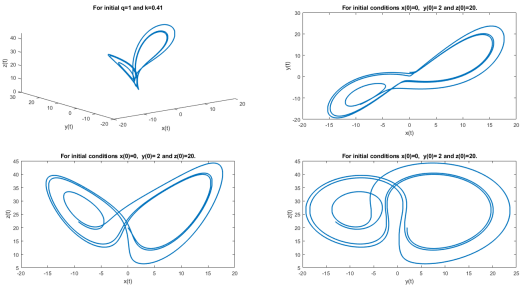

(f) For $q = 1$ and $k = 0.41$ (Example 2).

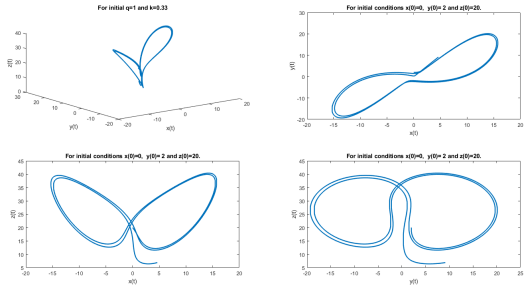

(g) For $q = 1$ and $k = 0.33$ (Example 2).

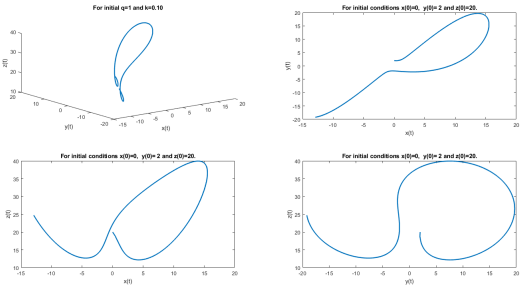

(h) For $q = 1$ and $k = 0.10$ (Example 2).

Figure 5. The dynamical behavior of the Lorenz chaotic system (6.1), using the Caputo-Fabrizio fractal-fractional derivative operator for different values of k and q.

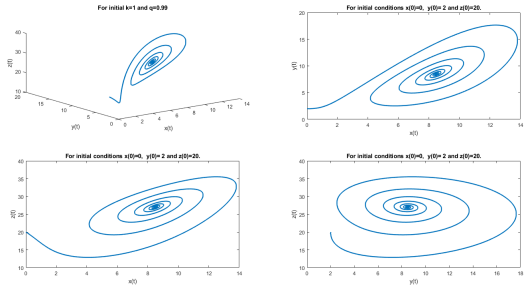

(a) For $k = 1$ and $k = 0.99$ (Example 2).

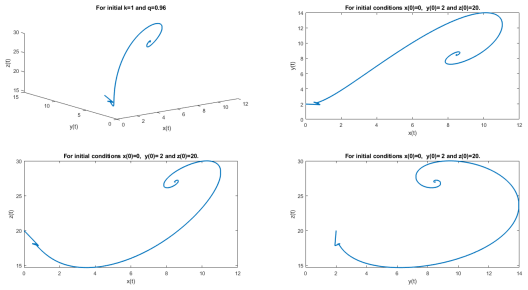

(b) For $k = 1$ and $q = 0.96$ (Example 2).

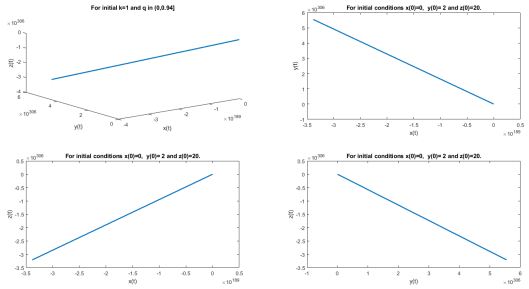

(c) For $k = 1$ and $0 < q \leq 0.94$ (Example 2).

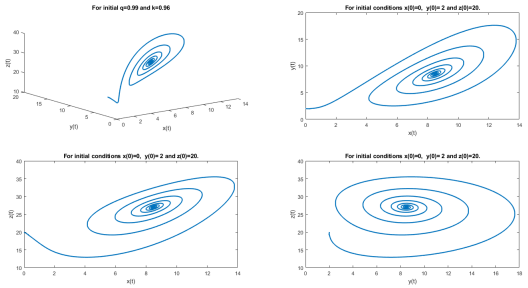

(d) For $q = 0.99$ and $k = 0.96$ (Example 2).

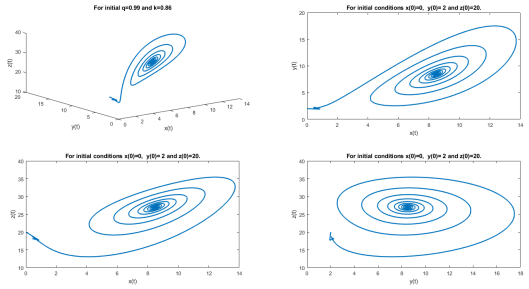

(e) For $q = 0.99$ and $k = 0.86$ (Example 2).

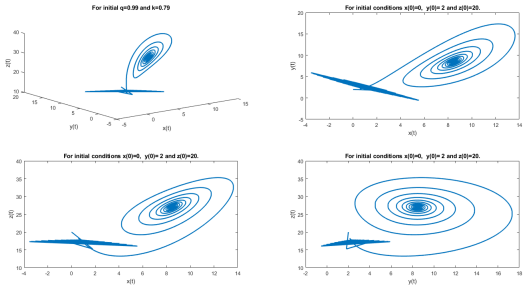

(f) For $q = 0.99$ and $k = 0.79$ (Example 2).

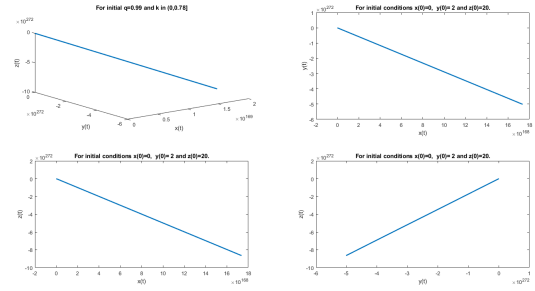

(g) For $q = 0.99$ and $0 < k \leq 0.78$ (Example 2).

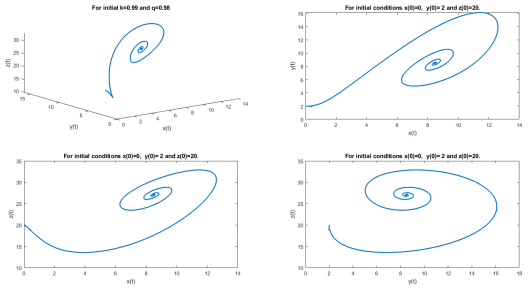

(h) For $k = 0.99$ and $q = 0.98$ (Example 2).

Figure 6. The dynamical behavior of the Lorenz chaotic system (6.1), using the Caputo-Fabrizio fractal-fractional derivative operator for different values of k and q.

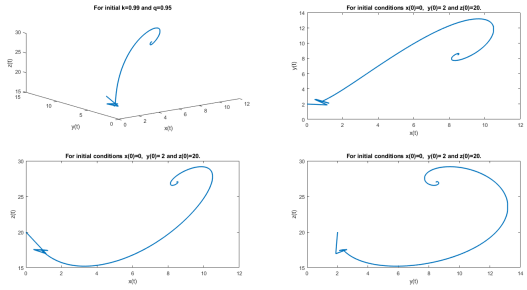

(a) For $k = 0.99$ and $k = 0.95$ (Example 2).

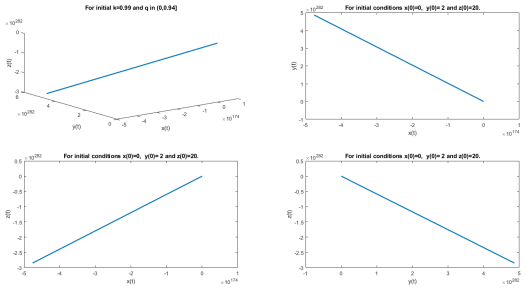

(b) For $k = 0.99$ and $0 < q \leq 0.94$ (Example 2).

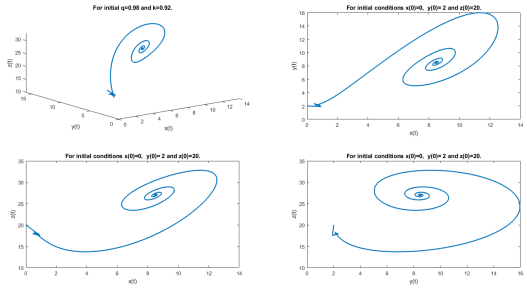

(c) For $q = 0.98$ and $k = 0.92$ (Example 2).

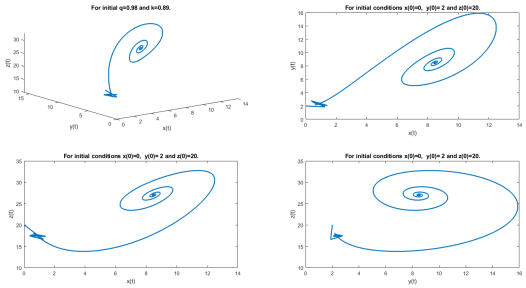

(d) For $q = 0.98$ and $k = 0.89$ (Example 2).

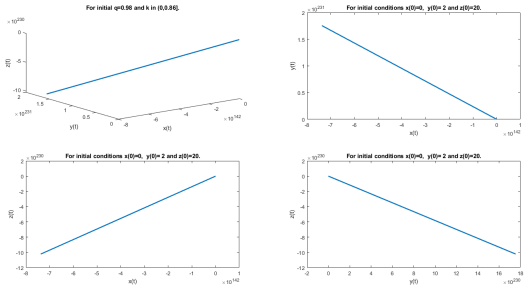

(e) For $q = 0.98$ and $0 < k \leq 0.86$ (Example 2).

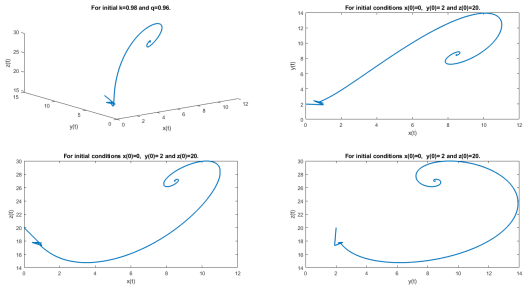

(f) For $k = 0.98$ and $q = 0.96$ (Example 2).

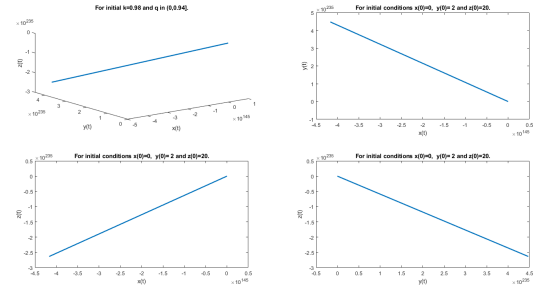

(g) For $k = 0.98$ and $0 < q \leq 0.94$ (Example 2).

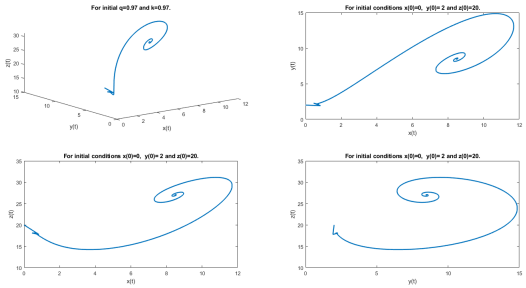

(h) For $q = 0.97$ and $k = 0.97$ (Example 2).

Figure 7. The dynamical behavior of the Lorenz chaotic system (6.1), using the Caputo-Fabrizio fractal-fractional derivative operator for different values of k and q.

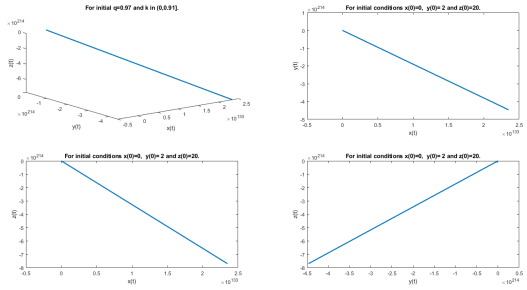

(a) For $q = 0.97$ and $0 < k \leq 0.91$ (Example 2).

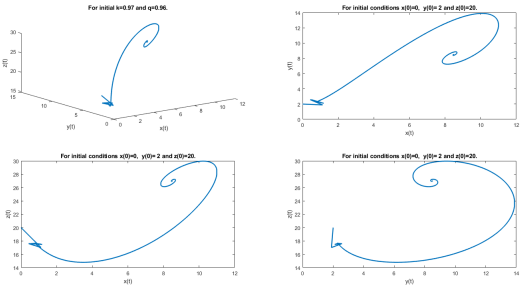

(b) For $k = 0.97$ and $q = 0.96$ (Example 2).

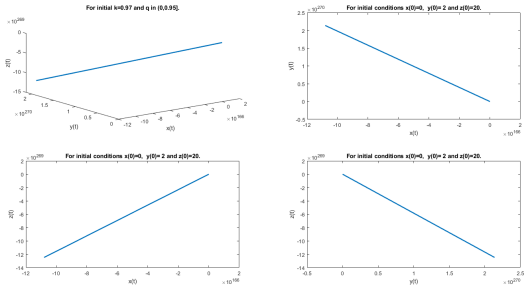

(c) For $k = 0.97$ and $0 < q \leq 0.95$ (Example 2).

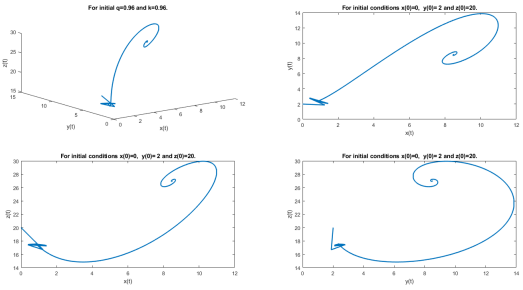

(d) For $q = 0.96$ and $k = 0.96$ (Example 2).

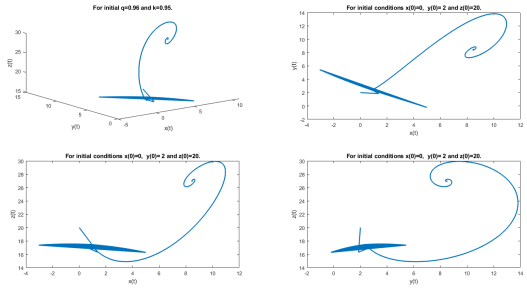

(e) For $q = 0.96$ and$k = 0.95$ (Example 2).

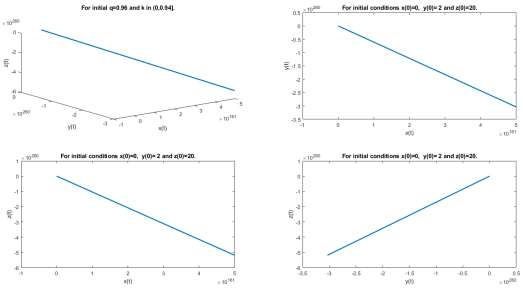

(f) For $q = 0.96$ and $0 < k \leq 0.94$ (Example 2).

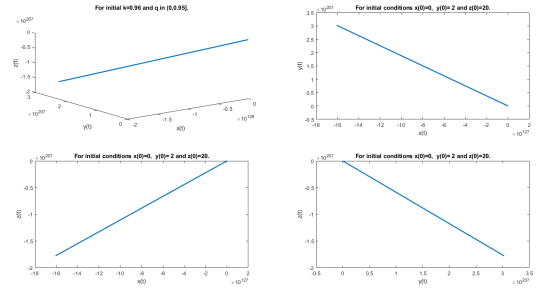

(g) For $k = 0.96$ and $0 < q \leq 0.95$ (Example 2).

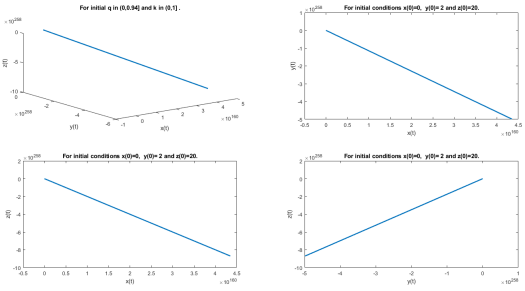

(h) For $0 < q \leq 0.94$ and $0 < k \leq 1$ (Example 2).

Figure 8. The dynamical behavior of the Lorenz chaotic system (6.1), using the Caputo-Fabrizio fractal-fractional derivative operator for different values of k and q.

7. Discussion

In Example 1 and 2, we modeled the Lorenz chaotic system with initial conditions $x(0) = y(0) = z(0) = -1$ and $x(0) = 0$, $y(0) = 2$ and $z(0) = 20$ respectively, using the Caputo-Fabrizio fractal-fractional derivative operator. We then solved the obtained nonlinear systems of equations using a numerical scheme for different fractal dimensions k and fractional order q. Figures 1–4 represent the graphical simulation, for example, 1, and Figures 5–8 represent the graphical simulation, for example 2. In both examples, we noticed that the fractal power $k = 1$ and the fractional power $q = 1$ recover the classical two-step Adams-Bashforth method and the classical differential and integral operators. Figures 1(a) and Figures 5(a) represents the graphical solutions for the case where $k = 1$ and $q = 1$ for example 1 and example 2, respectively. While solving the systems of equations, we noticed that for some values of k and q the solution blows up.

For both examples, we noticed that if we keep $q = 1$ and vary the value of k we can obtain graphical solutions for as far as $k = 0.10$, see Figures 1 and 5 but if we make $k = 1$ and vary the value of q the solution of the nonlinear system of equation blows up for some values of q. Keeping one variable constant and varying the others, we noticed that for the following values some values of k and q the solutions blow up, see Figure 2(d), 3(b), 3(d), 3(f), 3(h), 4(c)–(h) and for example 2, see Figure 6(c), 6(g), 7(b), 7(e), 7(g), 8(a), 8(c) and 8(f)–(h).

Taking into consideration that the chaotic systems are sensitive to initial conditions. Comparing the values for which the solution blows up between the two examples might give us an idea of the factors contributing to the blowing up of the solution. The following table shows a comparison of the values for which the solution blows up.

From Table 1, we can see that the solution for Example 1 for some values of k and q blows up faster than those in Example 2. This means that the choice of the initial conditions of the nonlinear system of equations also contributes to when the solution blows up for the nonlinear system under investigation.

Table 1. Comparison of the values for which the solution blows up for both examples.

Constant values	Example 1	Example 2
$k = 1$	$0 < q \leq 0.95$	$0 < q \leq 0.94$
$q = 0.99$	$0 < k \leq 0.81$	$0 < k \leq 0.78$
$k = 0.99$	$0 < q \leq 0.95$	$0 < q \leq 0.94$
$q = 0.98$	$0 < k \leq 0.89$	$0 < k \leq 0.86$
$k = 0.98$	$0 < q \leq 0.96$	$0 < q \leq 0.94$
$q = 0.97$	$0 < k \leq 0.94$	$0 < k \leq 0.91$
$k = 0.97$	$0 < q \leq 0.96$	$0 < q \leq 0.95$
$q = 0.96$	$0 < k \leq 0.96$	$0 < k \leq 0.94$
$k = 0.96$	$0 < q \leq 0.96$	$0 < q \leq 0.95$
$0 < k \leq 1$	$0 < q \leq 0.94$	$0 < q \leq 0.94$
$0 < q \leq 0.96$	$0 < k \leq 0.95$	$0 < k \leq 0.94$

7.1. Error estimate

In this section, we use numerical results obtained from the numerical scheme to estimate the rate of convergence using the following

$$p = \frac{\log\left|\frac{u^{\frac{h}{2}}-u^{h}}{u^{\frac{h}{4}}-u^{\frac{h}{2}}}\right|}{\log 2}$$

where $u^h = \{x^h(t), y^h(t), z^h(t)\}$, $u^{\frac{h}{2}} = \{x^{\frac{h}{2}}(t), y^{\frac{h}{2}}(t), z^{\frac{h}{2}}(t)\}$ and $u^{\frac{h}{4}} = \{x^{\frac{h}{4}}(t), y^{\frac{h}{4}}(t), z^{\frac{h}{4}}(t)\}$ are the approximate solutions to $u(x) = \{x(t), y(t), z(t)\}$ for the step size h, $\frac{h}{2}$ and $\frac{h}{4}$ respectively.

Table 2. The rate of convergence for different values of h using example 1.

h	$x(t)$	p
$\frac{1}{100}$	−1.230587514160928	1.904959580936555
$\frac{1}{200}$	−1.061110242113278	1.940190794821020
$\frac{1}{400}$	−1.015855771334397	1.961017182073904
$\frac{1}{800}$	−1.004063271904520	1.972167801697337
$\frac{1}{1600}$	−1.001034400255673	1.977926785981624
$\frac{1}{3200}$	−1.000262432420641	1.980853052009642
$\frac{1}{6400}$	−1.000066464983257	
$\frac{1}{12800}$	−1.000016818587168	

Table 3. The rate of convergence for different values of h using example 1.

h	$y(t)$	p
$\frac{1}{100}$	−2.326508213491328	1.067858535219673
$\frac{1}{200}$	−1.647800735475855	1.006794709692697
$\frac{1}{400}$	−1.324039249963567	0.992944397031469
$\frac{1}{800}$	−1.162919129852769	0.990829292631269
$\frac{1}{1600}$	−1.081964120101717	0.991036225398347
$\frac{1}{3200}$	−1.041228494373794	0.991461358994093
$\frac{1}{6400}$	−1.020733737952112	0.991752429070755
$\frac{1}{12800}$	−1.010425530442698	0.991914116840363
$\frac{1}{25600}$	−1.005241877425116	0.991995057252036
$\frac{1}{51200}$	−1.002635483703504	
$\frac{1}{102400}$	−1.001325035822124	

Table 4. The rate of convergence for different values of h using example 1.

h	$z(t)$	p
$\frac{1}{100}$	−0.810858602235998	1.134148250045712
$\frac{1}{200}$	−0.910831556058634	1.051723457397754
$\frac{1}{400}$	−0.956379615764291	1.020129659296684
$\frac{1}{800}$	−0.978351614908976	1.005880122139417
$\frac{1}{1600}$	−0.989185393271114	0.998981951425179
$\frac{1}{3200}$	−0.994580249280774	0.995555981083686
$\frac{1}{6400}$	−0.997279581417658	
$\frac{1}{12800}$	−0.998633411352176	

Table 5. The rate of convergence for different values of h using example 2.

h	$x(t)$	p
$\frac{1}{100}$	0.751972948680281	0.785531902054452
$\frac{1}{200}$	0.415109454355213	0.879128933122776
$\frac{1}{400}$	0.219682130799205	0.933763944099137
$\frac{1}{800}$	0.113429154201297	0.962477934907692
$\frac{1}{1600}$	0.057806699720829	0.977150215826183
$\frac{1}{3200}$	0.029262661073358	0.984573990764699
$\frac{1}{6400}$	0.014762798186914	
$\frac{1}{12800}$	0.007434930967961	

Table 6. The rate of convergence for different values of h using example 2.

h	$y(t)$	p
$\frac{1}{100}$	2.063882999678037	3.578639814091108
$\frac{1}{200}$	1.992390832959806	0.463370460207230
$\frac{1}{400}$	1.986406985255091	0.118777817473332
$\frac{1}{800}$	1.990747009184933	0.699165428640857
$\frac{1}{1600}$	1.994744030260617	0.865555010973675
$\frac{1}{3200}$	1.997205909082042	0.932675206008964
$\frac{1}{6400}$	1.998557074903865	
$\frac{1}{12800}$	1.999264931751799	

Table 7. The rate of convergence for different values of h using example 2.

h	$z(t)$	p
$\frac{1}{100}$	17.710724336596417	0.919794628750672
$\frac{1}{200}$	18.810610778750505	0.955734196405311
$\frac{1}{400}$	19.391993440099736	0.973775158693165
$\frac{1}{800}$	19.691742213503858	0.982881681370900
$\frac{1}{1600}$	19.844365880125473	0.987471151984859
$\frac{1}{3200}$	19.921588585883410	0.989778019827995
$\frac{1}{6400}$	19.960536712925116	
$\frac{1}{12800}$	19.980149246718597	

The results in Tables 2–7 depict order one and two rate of convergence. However, this approach might not be entirely reliable because we deal with chaotic systems that are extremely sensitive to initial conditions. Some other methods are proposed in [49, 50].

8. Conclusions

In this study, we used the newly proposed Caputo Fabrizio fractal fractional operator with different fractal dimension k and fractional order q, to capture and analyze the dynamical behavior of the Lorenz chaotic system. We present the numerical scheme used to solve the system of nonlinear equations and obtained graphical numerical simulations for different values of q and k. We noticed that for the fractal dimension $k = 1$ and fractional order $q = 1$ we obtain a two-step Adams Bashforth method and the classical differential and integral operators. We also noticed that for some values of q and k the solutions blow up. Taking into consideration that the chaotic systems are sensitive to initial conditions we compared two examples of the same nonlinear system of equations with different initial conditions, we noticed that the choice of the initial conditions also affect when some solutions blow up. For future work, we want to find out what other factors contribute to the blowing up of the solutions for some values of q and k.

Acknowledgments

The authors are grateful to the referees for providing valuable comments and helpful suggestions on the paper.

Conflict of interest

The authors declare no conflict of interest.

References

1. R. E. Gutierrez, J. M. Rosario, J. Tenreiro Machado, Fractional order calculus: basic concepts and engineering applications, *Math. Probl. Eng.*, **2010** (2010), 375858.
2. M. Inc, A. Yusuf, A. I. Aliyu, D. Baleanu, Investigation of the logarithmic-KdV equation involving Mittag-Leffler type kernel with Atangana–Baleanu derivative, *Physica A*, **506** (2018), 520–531.
3. R. Almeida, N. R. Bastos, M. T. T. Monteiro, Modeling some real phenomena by fractional differential equations, *Math. Method. Appl. Sci.*, **39** (2016), 4846–4855.
4. R. Almeida, A. B. Malinowska, M. T. T. Monteiro, Fractional differential equations with a Caputo derivative with respect to a kernel function and their applications, *Math. Method. Appl. Sci.*, **41** (2018), 336–352.
5. A. Yusuf, S. Qureshi, M. Inc, A. I. Aliyu, D. Baleanu, A. A. Shaikh, Two-strain epidemic model involving fractional derivative with Mittag-Leffler kernel, *Chaos*, **28** (2018), 123121.
6. M. Awadalla, Y. Yameni, Modeling exponential growth and exponential decay real phenomena by ψ-Caputo fractional derivative, *JAMCS*, **28** (2018), 1–13.
7. A. Jajarmi, S. Arshad, D. Baleanu, A new fractional modelling and control strategy for the outbreak of dengue fever, *Physica A*, **535** (2019), 122524.
8. M. Khader, K. M. Saad, Numerical treatment for studying the blood ethanol concentration systems with different forms of fractional derivatives, *Int. J. Mod. Phys. C*, **31** (2020), https://doi.org/10.1142/S0129183120500448.
9. S. Bushnaq, S. A. Khan, K. Shah, G. Zaman, Existence theory of HIV-1 infection model by using arbitrary order derivative of without singular kernel type, *Journal of Mathematical Analysis*, **9** (2018), 16–28.
10. S. Rezapour, H. Mohammadi, A study on the AH1N1/09 influenza transmission model with the fractional Caputo–Fabrizio derivative, *Adv. Differ. Equ.*, **2020** (2020), 1–15.
11. S. B. Chen, S. Rashid, M. A. Noor, R. Ashraf, Y. M. Chu, A new approach on fractional calculus and probability density function, *AIMS Mathematics*, **5** (2020), 7041–7054.
12. S. Das, I. Pan, *Fractional order signal processing: introductory concepts and applications*, Springer Science & Business Media, 2011.
13. F. Meral, T. Royston, R. Magin, Fractional calculus in viscoelasticity: an experimental study, *Commun. Nonlinear Sci.*, **15** (2010), 939–945.
14. K. M. Owolabi, A. Atangana, On the formulation of Adams-Bashforth scheme with Atangana-Baleanu-Caputo fractional derivative to model chaotic problems, *Chaos*, **29** (2019), 023111.
15. M. Inc, A. Yusuf, A. I. Aliyu, D. Baleanu, Investigation of the logarithmic-KdV equation involving Mittag-Leffler type kernel with Atangana–Baleanu derivative, *Physica A*, **506** (2018), 520–531.
16. A. Atangana, A. Akgül, K. M. Owolabi, Analysis of fractal fractional differential equations, *Alex. Eng. J.*, **59** (2020), 1117–1134.
17. A. Akgül, A novel method for a fractional derivative with non-local and non-singular kernel, *Chaos Soliton. Fract.*, **114** (2018), 478–482.
18. K. M. Owolabi, A. Atangana, Chaotic behaviour in system of noninteger-order ordinary differential equations, *Chaos Soliton. Fract.*, **115** (2018), 362–370.
19. K. M. Owolabi, Z. Hammouch, Spatiotemporal patterns in the Belousov–Zhabotinskii reaction systems with Atangana–Baleanu fractional order derivative, *Physica A*, **523** (2019), 1072–1090.

20. D. Mathale, E. F. Doungmo Goufo, M. Khumalo, Coexistence of multi-scroll chaotic attractors for fractional systems with exponential law and non-singular kernel, *Chaos Soliton. Fract.*, **139** (2020), 110021.
21. E. F. Doungmo Goufo, Mathematical analysis of peculiar behavior by chaotic, fractional and strange multiwing attractors, *Int. J. Bifurcat. Chaos*, **28** (2018), 1850125.
22. I. Podlubny, *Fractional differential equations: an introduction to fractional derivatives, fractional differential equations, to methods of their solution and some of their applications*, Elsevier, 1998.
23. E. F. Doungmo Goufo, J. J. Nieto, Attractors for fractional differential problems of transition to turbulent flows, *J. Comput. Appl. Math.*, **339** (2018), 329–342.
24. S. Eftekhari, A. Jafari, Numerical simulation of chaotic dynamical systems by the method of differential quadrature, *Sci. Iran.*, **19** (2012), 1299–1315.
25. E. F. Doungmo Goufo, The Proto-Lorenz system in its chaotic fractional and fractal structure, *Int. J. Bifurcat. Chaos*, **30** (2020), 2050180.
26. E. F. Doungmo Goufo, Y. Khan, A new auto-replication in systems of attractors with two and three merged basins of attraction via control, *Commun. Nonlinear Sci.*, **96** (2021), 105709.
27. E. F. Doungmo Goufo, Multi-directional and saturated chaotic attractors with many scrolls for fractional dynamical systems, *Discrete Cont. Dyn. S*, **13** (2020), 629–643.
28. E. F. Doungmo Goufo, Fractal and fractional dynamics for a 3D autonomous and two-wing smooth chaotic system, *Alex. Eng. J.*, **59** (2020), 2469–2476.
29. Y. Mousavi, A. Alf, Fractional calculus-based firefly algorithm applied to parameter estimation of chaotic systems, *Chaos Soliton. Fract.*, **114** (2018), 202–215.
30. M. Fiaz, M. Aqeel, Fractional order analysis of modified stretch–twist–fold flow with synchronization control, *AIP Adv.*, **10** (2020), 125202,
31. Q. Jia, Hyperchaos generated from the Lorenz chaotic system and its control, *Phys. Lett. A*, **366** (2007), 217–222.
32. Y. Yu, H. X. Li, S. Wang, J. Yu, Dynamic analysis of a fractional-order Lorenz chaotic system, *Chaos Soliton. Fract.*, **42** (2009), 1181–1189.
33. H. T. Yau, J. J. Yan, Design of sliding mode controller for Lorenz chaotic system with nonlinear input, *Chaos Soliton. Fract.*, **19** (2004), 891–898.
34. E. N. Lorenz, Deterministic nonperiodic flow, *J. Atmos. Sci.*, **20** (1963), 130–141.
35. A. Azam, M. Aqeel, S. Ahmad, F. Ahmad, Chaotic behavior of modified stretch-twist-fold (STF) flow with fractal property, *Nonlinear Dyn.*, **90** (2017), 1–12.
36. T. Zhou, Y. Tang, G. Chen, Chen's attractor exists, *Int. J. Bifurcat. Chaos*, **14** (2004), 3167–3177.
37. O. E. Rössler, An equation for continuous chaos, *Phys. Lett. A*, **57** (1976), 397–398.
38. L. Zhou, F. Chen, Sil'nikov chaos of the Liu system, *Chaos*, **18** (2008), 013113.
39. A. Atangana, Fractal-fractional differentiation and integration: connecting fractal calculus and fractional calculus to predict complex system, *Chaos Soliton. Fract.*, **102** (2017), 396–406.
40. M. Giona, Fractal calculus on [0, 1], *Chaos Soliton. Fract.*, **5** (1995), 987–1000.
41. J. Fan, J. He, Fractal derivative model for air permeability in hierarchic porous media, *Abstr. Appl. Anal.*, **2012** (2012), 354701.
42. Y. Hu, J. H. He, On fractal space-time and fractional calculus, *Therma. Sci.*, **20** (2016), 773–777.

43. S. Qureshi, A. Atangana, Fractal-fractional differentiation for the modeling and mathematical analysis of nonlinear diarrhea transmission dynamics under the use of real data, *Chaos Soliton. Fract.*, **136** (2020), 109812.
44. H. Srivastava, K. M. Saad, Numerical simulation of the fractal-fractional Ebola Virus, *Fractal Fract.*, **4** (2020), 49.
45. A. Atangana, S. Qureshi, Modeling attractors of chaotic dynamical systems with fractal–fractional operators, *Chaos Soliton. Fract.*, **123** (2019), 320-337.
46. E. F. Doungmo Goufo, Chaotic processes using the two-parameter derivative with non-singular and non-local kernel: basic theory and applications, *Chaos*, **26** (2016), 084305.
47. A. Atangana, D. Baleanu, New fractional derivatives with nonlocal and non-singular kernel: theory and application to heat transfer model, 2016, *arXiv:1602.03408*.
48. A. Atangana, I. Koca, Chaos in a simple nonlinear system with Atangana–Baleanu derivatives with fractional order, *Chaos Soliton. Fract.*, **89** (2016), 447–454.
49. J. C. B. de Figueiredo, L. Diambra, C. P. Malta, Convergence criterium of numerical chaotic solutions based on statistical measures, *Applied Mathematics*, **2** (2011), 436–443.
50. Y. S. Shimizu, K. Fidkowski, Output-based error estimation for chaotic flows using reduced-order modeling, *2018 AIAA Aerospace Sciences Meeting*, 2018. Available from: https://arc.aiaa.org/doi/abs/10.2514/6.2018-0826.

AIMS Press